

Effects of Boundary Conditions on Magnetic Friction

Kentaro Sugimoto

Department of Physics, The University of Tokyo

December 20, 2017

I would like to express my deepest gratitude to Prof. Naomichi Hatano whose enormous support and insightful comments were invaluable during the course of my study. I am also indebt to Ryo Tamura who provided technical help and sincere encouragement. I would also like to express my gratitude to my family for their moral support and warm encouragements.

Abstract

In the present thesis, hogehoge. Moreover, fugafuga.

Contents

1	Introduction	7
1.1	Sliding Frictions as Non-Equilibrium Problems	8
1.2	Impossibility of the Observation of the Sliding Surface	9
1.3	Manipulating the Friction	9
1.4	Magnetic Friction	10
2	Velocity-driven Non-equilibrium Phase Transition in Ising Models	13
3	Numerical Simulations	17
3.1	Setup of the Model	17
3.2	Definitions of Physical Quantities	19
3.3	Non-equilibrium Monte Carlo Simulation	21
3.3.1	Introduction the Time Scale to Ising Models	21
3.3.2	Slip Plane with the Velocity v	23
3.3.3	Calculation Method	23
4	Results of Simulations	25
4.1	Frictional Force Density $f(L_z, T)$	26
4.2	Bulk Energy Density $\epsilon_b(L_z, T)$	28

5	Summary and Discussion	31
A	Analysis based on Stochastic Matrices	33
A.1	A Simple Example: Stochastic Ising Model with N -spins	34
A.2	General Theory of Stochastic Matrices	35
A.2.1	Construction of the Stochastic Matrix based on the Detailed Balanced Condition	48
A.3	Stochastic Matrices and Non-Equilibrium Monte Carlo Simulations	48
A.4	Calculation Non-Equilibrium Observables by the Stochastic Matrices	48
B	Results of Simulations in More Detail	49
B.1	Checking the Convergence in the Limit $L_x \rightarrow \infty$	49
B.1.1	Dependence of $F(L_x, L_z, T)/L_x$ on L_x for each L_z	51
B.1.2	Dependence of $E_b(L_x, L_z, T)/(L_x L_z)$ on L_x for each L_z	51
B.2	Time Series of Observables	51
B.2.1	title	51

Chapter 1

Introduction

The sliding friction in solids is a too complex problem to deal with, despite the fact that our daily lives are linked with it in various forms. One reason is that there is no general theory for various and a number of physical degrees of freedom, which determines the most important degree for the sliding friction as a phenomenon.

One may think that, with the skill of statistical mechanics, we can deal with the problem in a systematic manner. But there still remains several problems as follows:

- **Problem1:** The sliding friction is essentially non-equilibrium phenomenon.
- **Problem2:** We cannot directly observe the sliding surface.

In this chapter we introduce two of the most famous problems with dealing the frictional force as the problem of statistical mechanics. We give recent developments for solving these problems. We then propose the question related to a problem about the *manipulation* of the sliding friction which occurs in highly lubricated solids. To this end we simplify the problem into a dimensional crossover in lattice systems.

1.1 Sliding Frictions as Non-Equilibrium Problems

We can regard the sliding friction as follows in an elementary manner. We consider an object O and a substrate S , and let S slide against O with them contacting and an external force. When O and S interact with each other, the kinetic energy of O given by the external force is expected to lose by the interaction, and then the entire system $O + S$ heats up (if they form a closed system) or an energy dissipation occurs from the system to external environment (if they form an open system). In the latter case, under the assumption that the dissipation process stationarily occurs, the frictional force f_{fric} take a constant value balancing with the external force. This setup is realized when we keep the external force f_{ext} so that the sliding velocity v take a constant value. Then the frictional force f_{fric} is dealt with as a function of the sliding velocity as $f_{\text{fric}} = f_{\text{fric}}(v)$.

The traditional way of statistical mechanics, called the linear response theory, appears to deal with the problem under the condition that the velocity v is much smaller than the rate ξ/τ , where ξ and τ are the characteristic length and time of the system. But we already know well the phenomenon that the static frictional force is non-zero value for several systems. In such systems, we easily observe the non-linearity of the frictional force f_{fric} for the velocity v . This simply shows us the complexity of the problem which cannot be captured by applying the traditional way.

Many researches have dealt with the problem using the numerical way or limiting to an extreme region of parameters to avoid attack with the perturbative way.

1.2 Impossibility of the Observation of the Sliding Surface

The dimensionality of the sliding surface is up to two-dimension, if that of the whole system is the three-dimension. Sliding surfaces of such systems are different in many ways from well-known two-dimensional surfaces of three-dimensional solids which have investigated for many years, then we cannot perform a direct observation of the sliding surface by apparatuses such as microscopes. The difficulty prevents us from revealing non-equilibrium properties of the sliding friction.

There is the way to observe the contact plane with the microscope and an optically transparent matter, but most researches avoid a direct observations by measuring other observables to indirectly observe the contact plane.

1.3 Manipulating the Friction

Recent researches well revealed the nature of sliding frictions. This also leads us to conflict with a new problems about the friction in atomically microscopic systems.

Ordinary frictions in solids are mostly governed by excitations of phonon degrees of freedom, because the contact plane is almost always rough than the scale of the atom. But once we get the contact plane highly lubricated, other degrees of freedom, such as the orbital and the spin of electrons, emerges as the main contribution to the friction, in addition to the phonon excitation.

We are already familiar with the most remarkable example of such a system in our daily lives, which is called *micro electric mechanical system* (**MEMS**). MEMS plays an important role in the head of inkjet printers, the accelerometer in smartphones and so on. As an aspect of the MEMS, there are processed planes with an accuracy of a micrometer or a nanometer

and they are also moving parts. Thus they inevitably experience the new type of the friction by operations. In addition the smaller size of these systems makes the problem more serious, because the rate of the surface area over the volume of a system become larger with the smaller size in general.

Thus we have to tackle with the issue of manipulation the friction in such a smaller system by getting more fundamental knowledges of the friction.

1.4 Magnetic Friction

The way to manipulate the friction in such a small system is less understood than its nature. Thus we consider the manipulation of magnetic materials as an easier problem to analyze by lattice models and its simulations.

Frictions in such models themselves are a new type of the problem problems, and date back to the numerical research by Kadau et al. [2]. They have revealed that two square lattices of a Ising model which slide with each other experience the friction, depending on the temperature and the sliding velocity, by Monte Carlo simulations. Immediately after the research, it was revealed that the Ising model goes to a non-trivial non-equilibrium phase transitions (**NEPT**) in the high-velocity limit, where the two sliding models are decoupled in terms of the correlation between the two models and feel a mean field depending the magnetization of each other [1]. By this treatment, we are able to access the novel critical point which is located in a higher temperature than the ordinal critical point in general for models with arbitrary dimensions and geometries (see Chapter 2). In addition to the results, they developed a new algorithm which enables the analytical treatment in more detail and revealed the non-equilibrium critical point for arbitrary velocities.

Based on their results [1], we consider a dimensional crossover from one-dimension to two in

Ising models with two fixed boundary conditions. In the one-dimensional limit the boundary conditions seem to have the most effect on the friction, whereas in the two-dimensional limit there seems to be no effects. Behaviors in the both limits for the free boundary condition correspond to the results [1]. In this way we think the problem of the manipulation as the dimensionality with different boundary conditions. Simpler boundary conditions would be realized by experiments with the boundary spins of relatively moving magnets aligned.

Chapter 2

Velocity-driven Non-equilibrium Phase Transition in Ising Models

To discuss the non-equilibrium crossover between two different dimensions, we have to make a brief review the exact results [1] by Hucht. Their analysis is based on the fact that two Ising cylinders with relative motion make a novel mean field and they lead the system to non-trivial phase transition.

We now consider two equivalent square lattices of Ising model each of which contacts with the other by one of its one-dimensional boundary. If we leave two models alone, we can regard the models as an Ising model with a twice the size. With the coupling to the heat bath, we expect the model thermalize. But one of the couple are moving along the contact plane with a constant velocity v , the entire model goes into a non-equilibrium stationary state, instead of thermalization. The non-equilibrium stationary state well describes the behavior of two magnetic materials are sliding with the friction. This setup are explained in detail in Chapter 3.

The two dimensional Ising model has the phase transition which occurs at the critical

temperature $T_c = \text{exact value or equation form}$ in the thermodynamical limit $N/V \rightarrow \infty$ with $N/V = \text{const.}$, where N is the number of spins and V is the volume of the system as a well known fact. The model which we consider in this chapter is no exception, if the sliding velocity v is set to zero. The result [1] claims that the critical temperature T_c *branches* at the point $v = 0$ towards the limit $v = \infty$. The system exhibits the ordinary phase transition at the vertical line $T = T_c(v = 0)$, whereas exhibits a novel phase transition at the curve $T = T_c(v > 0)$ where the magnetization grows up near the contact plane rather than the rest *cite the phase diagram of the ref.* These phenomena were first reported in the numerical results [2] by Kadau et al. using Monte Carlo simulations with both Metropolis algorithms and Glauber algorithms in two-dimensional models, and then investigated in more exact manner [1] by Hucht in several dimensions and model geometries. One of the important point in the latter result is that for $v \rightarrow 0$ we can write the closed exact equation for the *second* critical temperature $T_c(v > 0)$. In addition it is also important that a novel algorithm, called *multiplicative rate*, enabled us to give the equation for $T_c(v > 0)$ which fully depends on the algorithm for arbitrary $v > 0$.

If the velocity v is much less than the rate $\xi_x^{(\text{eq})}(\beta)/\tau_x^{(\text{eq})}(\beta)$, we can expect the system to behave well similarly to its equilibrium state. We denote the correlation length along the direction parallel to the contact plane by $\xi_x^{(\text{eq})}(\beta)$ and the correlation time by $\tau_x^{(\text{eq})}(\beta)$ respectively for the equilibrium state of an inverse temperature $\beta := (k_B T)^{-1}$. This corresponds to the circumstance that the pumped energy by the constant sliding is most quickly relaxed towards the heat bath. In the case, the structure of domain walls near the contact plane is well sustained. On the other hand, the velocity v much greater than the rate $\xi_x^{(\text{eq})}(\beta)/\tau_x^{(\text{eq})}(\beta)$ will lead the system to a stationary state much far from equilibrium, then the structure near the contact plane will be destroyed.

In the latter case that the velocity is much higher, a mean field picture that two sets of the

moving spins along the contact plane act on the other *relatively* moving spins as the spatially-averaged effective field. In other words, the magnetization of one half of the system corresponds the effective field of the other, and vice versa. This enables us to write a self-consistent equation for the temperature $T_c(v \rightarrow \infty)$.

We summarize the result for one-dimensional chains and that of two-dimensional planes, in order to discuss the crossover from one-dimension to two-dimension in our models in Chapter 5.

Brief review.

Chapter 3

Numerical Simulations

3.1 Setup of the Model

Sliding friction is a form of energy dissipation on the surface between a moving object and its substrate. The dissipated energy is originated in the kinetic energy of the moving object. We here consider constantly moving case in which an external force maintains the motion of the object with endless supply of its kinetic energy. This view leads to its *non-equilibrium stationary state*. When the system is in a non-equilibrium stationary state, it is often easy to calculate several *energy currents* such as the frictional heat, its power and so on. Applying the view to our case where two square lattices of the Ising model slide against each other, we can formulate the problem as follows.

1. We prepare a square lattice of the Ising model of size $L_x \times L_z$ and impose periodic boundary conditions in the transverse (x) direction. We first set the system in the equilibrium state of a temperature T , whereas we set the open boundary conditions in the longitudinal (z) direction for the moment (fig).
2. We cut the system along the x -direction into two parts, maintaining interactions on the

cut (fig).

3. We slide two parts along the cut plane with relative velocity v . In other words, we shift the upper half by a lattice constant every $1/v$ unit time.

The Hamiltonian of the system is given by

$$\hat{H} = \hat{H}_{\text{upper}} + \hat{H}_{\text{lower}} + \hat{H}_{\text{slip}}(t), \quad (3.1)$$

where

$$\hat{H}_{\text{upper}} := -J \sum_{\langle i,j \rangle \in \text{upper}} \hat{\sigma}_i \hat{\sigma}_j, \quad (3.2)$$

$$\hat{H}_{\text{lower}} := -J \sum_{\langle i,j \rangle \in \text{lower}} \hat{\sigma}_i \hat{\sigma}_j, \quad (3.3)$$

$$\hat{H}_{\text{slip}}(t) := -J \sum_{\langle i,j(t) \rangle \in \text{slip}} \hat{\sigma}_i \hat{\sigma}_{j(t)}, \quad (3.4)$$

where *upper*, *lower* and *slip* represent the set of interacting spin pairs the upper half, the lower half and the slip plane of the entire system. Shift operations lead the system to repeated *pumping* and *dissipation* processes as follows:

1. **Shifting:** A shift operation excites the energy on the slip plane by the ammount $\langle \hat{H}_{\text{slip}}(t') - \hat{H}_{\text{slip}}(t) \rangle_{\text{st}}$. The letter t' denotes the time just after the shift operation from the time t .

2. **Relaxing-1:** The excited energy on the slip plane dispenses to the entire system $\langle \hat{H}_{\text{upper}} + \hat{H}_{\text{lower}} + \hat{H}_{\text{slip}}(t) \rangle_{\text{st}}$.
3. **Relaxing-2:** The excited entire system relaxes toward the equilibrium the heat bath.

We defined the stationary state average $\langle \hat{A} \rangle_{\text{st}} := \sum_i A_i p_i^{(\text{st})}$ for an arbitrary observable \hat{A} , where $\{A\}_i$ are eigenvalues of \hat{A} and $\{p_i^{(\text{st})}\}$ are stationary state probability distribution. Note that the distribution $\{p_i^{(\text{st})}\}$ are quite different from the equilibrium (canonical) probability distribution $p_i^{(\text{eq})} \propto \exp[-E_i/k_B T]$. In addition, the distribution $\{p_i^{(\text{st})}\}$ depends on the sliding velocity v , and therefore it has infinite number of families.

The excited and relaxed amounts of energy per unit time correspond to the energy pumping and dissipation, respectively. The energy pumping $P(t)$ and dissipation $D(t)$ are given by

$$P(t) := \sum_{i_v=0}^{v-1} \left\langle \hat{H}_{\text{slip}} \left(t' - 1 + \frac{i_v}{v} \right) - \hat{H}_{\text{slip}} \left(t - 1 + \frac{i_v}{v} \right) \right\rangle_{\text{st}}, \quad (3.5)$$

$$D(t) := \sum_{i_v=0}^{v-1} \left\langle \hat{H}_{\text{slip}} \left(t - 1 + \frac{i_v + 1}{v} \right) - \hat{H}_{\text{slip}} \left(t' - 1 + \frac{i_v}{v} \right) \right\rangle_{\text{st}}. \quad (3.6)$$

3.2 Definitions of Physical Quantities

We now consider the case in which that the system is in a non-equilibrium stationary state.

We define the frictional force density $f(L_z, T)$ by

$$f(L_z, T) := \lim_{L_x \rightarrow \infty} \frac{F(L_x, L_z, T)}{L_x}, \quad (3.7)$$

where $F(L_x, L_z, T)$ is the frictional force of a system of size $L_x \times L_z$ at a temperature T . We numerically formulate the large-size limit $L_x \rightarrow \infty$ as follows.

———— Numerical large-size limit $L_x \rightarrow \infty$ ————

If the quantity $F(L_x, L_z, T)/L_x$ is independent on L_x , $F(L_x, L_z, T)/L_x$ is a good approximation for $f(L_z, T)$.

In numerical simulations, we calculate the frictional force $F(L_x, L_z, T)$ using its power $D(L_x, L_z, T)$ by the formula

$$F(L_x, L_z, T) = \frac{D(L_x, L_z, T)}{v}, \quad (3.8)$$

where the quantity $D(L_x, L_z, T)$ is the long-time limit of $D(t)$ for the lattice of $L_x \times L_z$ at a temperature T .

We can easily verify the formula (3.8) by considering general cases in which the frictional force and its power are both time dependent. Denoting the frictional force $F(x)$ at the position x , it holds that

$$\int_{t_0}^{t_1} dt D(t) = \int_{x(t_0)}^{x(t_1)} dx F(x) = \int_{t_0}^{t_1} \frac{dx}{dt} dt F(x(t)) = v \int_{t_0}^{t_1} dt F(x(t)), \quad (3.9)$$

for a time dependent $D(t)$, because $dx/dt = v$. Under the assumption of a non-equilibrium stationary state, in the long-time limit, the integrands in both hand sides of the relation (3.9) are still equal to each other, and hence

$$D(L_x, L_z, T) = vF(L_x, L_z, T). \quad (3.10)$$

From now we call the quantity $D(L_x, L_z, T)$ *energy dissipation*.

Our models always reach non-equilibrium stationary states in the long-time limit $t \rightarrow \infty$, which depend on the temperature T and the sliding velocity v ; We will prove in App. A. We

use the fact that $\lim_{t \rightarrow \infty} |D(t)| = \lim_{t \rightarrow \infty} |P(t)|$ in order to calculate average value \bar{D} with less fluctuation by using the value \bar{P} [3–5]. We therefore have

$$P(L_x, L_z, T) = vF(L_x, L_z, T). \quad (3.11)$$

We also define the bulk energy density $\epsilon_b(L_z, T)$ as follows

$$\epsilon_b(L_z, T) := \lim_{L_x \rightarrow \infty} \frac{E_b(L_x, L_z, T)}{L_x L_z}, \quad (3.12)$$

where $E_b(L_x, L_z, T)$ is the energy of entire system. Straightforwardly, we define the bulk heat capacity $c_b(L_z, T)$ as follows

$$c_b(L_z, T) := \frac{\partial \epsilon_b(L_z, T)}{\partial T}. \quad (3.13)$$

3.3 Non-equilibrium Monte Carlo Simulation

Energy dissipation process towards the heat bath occurs via a spin flip. This fundamental processes do not only describe equilibrium states, but also non-equilibrium stationary states for a fixed temperature T [6]. Using Monte Carlo method, we can simulate this process.

3.3.1 Introduction the Time Scale to Ising Models

The Ising model which we deal with is a kind of kinetic Ising models [6], in which its time dependent statistics plays several important roles. In order to calculate dynamical observables such as the frictional power (3.11) and its dissipation rate (3.8), we have to define *a unit time* for finite size systems. We now consider the case in which a homogeneous spin chain of

the volume L and a heat bath with the temperature T are interacting. This system are well described with enough large number of the spins. Denoting such a number N , we can consider two macroscopically equivalent models as follows:

- An N -spin chain with the lattice constant $a = L/N$,
- An $(M \times N)$ -spin chain with the lattice constant $a = L/(M \times N)$,

where M is the large number which have the same property as N . Since both of models well describe the system of volume L , typical time scale¹ of each system should be the same. And under the *homogeneous* assumption that for both models each spin is independently interacting with the heat bath, the dynamics of any spin in the former and that of any M -spins subsystem in the latter are effectively equivalent. Thus as long as we consider the dynamics of same volume systems, we can define the unit time scale using its number of spins. This concept can be easily implemented on the ordinary *equilibrium* Monte Carlo simulation for classical spin systems.

For the equilibrium Monte Carlo simulation, the most naive approach for the equilibrium state is the single flip algorithm, where we perform the sequence a random selection of the spin and its flipping with temperature dependent probability $p(T)$. We often use the Metropolis probability $p_M(T) := \min\{1, e^{-\frac{\Delta E}{k_B T}}\}$ as the probability $p(T)$, where ΔE is the energy difference by the flipping. The Metropolis probability $p_M(T)$ have a good property, called *detailed balanced condition*, which certainly leads the system towards the true equilibrium state with enough many repetition of the algorithm. This process and randomness well describes the interaction and the homogeneousness with the heat bath. We often call *Monte Carlo step* a single process of the algorithm, and define *Monte Carlo sweep* N -times process, where N is the number of

¹If we use the same criterion, any time scale may be introduced. For example, we can define a *typical time scale* as the time taken to flip all the spin.

spins. According to the earlier discussion, the unit time in the system is nothing but the Monte Carlo sweep. Thus the more spins the system contains, the higher time resolution we can simulate with.

3.3.2 Slip Plane with the Velocity v

Using the introduced time scale, we can also introduce the slip plane with the velocity v to the system with N -spins. Corresponding to the setup in Sec. 3.1, we perform the extended single flip algorithm as follows:

1. **Shifting:** We shift the upper half by a lattice constant.
2. **Flipping:** We perform ordinary single flips for N/v times.
3. We repeat the process 1 + 2 for $(v - 1)$ times.

In the extended algorithm, the upper half slides with the velocity v in a unit time at regular intervals. We proved the fact that this algorithm lead the system of any size to the non-equilibrium stationary state depending the temperature T and the velocity v (see appendix A in detail).

3.3.3 Calculation Method

The observables which we are interested in are the frictional power $P(t)$ and its dissipation rate $D(t)$. In Monte Carlo simulations, the frictional power $P(t)$ and the dissipation rate $D(t)$ are the energy difference by the shifting operation and that by the flipping respectively, for a unit time. Both observables have the same absolute value in the long time limit.

Chapter 4

Results of Simulations

In this chapter, we show the results of the Monte Carlo simulation of two-dimensional Ising models. To discuss the dependence of the frictional force density $f(L_z, T)$ and the bulk energy density $\epsilon_b(L_z, T)$ on the size L_z and the temperature T with the fixed velocity $v = 10$, we performed the numerical large size limit $L_x \rightarrow \infty$ with the fixed L_z and T (see appendix B.1). To get the observables in the non-equilibrium stationary state, we performed the equilibration process for 5000 sweeps and the stationarization process for 5000 sweeps for all given parameters. The convergence of the observables to the equilibrium value and the stationary value for these time regions respectively are checked carefully (see appendix B.2).

The range of parameters in our simulation is as follows. We computed the value of $f(L_z, T)$ for temperatures $k_B T/J \in \{0.0, 0.1, 0.2, \dots, 1.9, 2.0, 2.02, 2.04, \dots, 2.48, 2.50, 2.6, 2.7, \dots, 5.0\}$, sizes $L_z \in \{4, 6, 8, 10, 12, 14, 16\}$ and these for the two boundary conditions, the anti-parallel and the parallel. For the anti-parallel boundary the initial state is set to the domain-wall state, where spin variables σ_i in the upper half of the system are the same value as the upper boundary, and in the lower half as the lower boundary. For the parallel boundary the initial state is set to the magnetized state, where all spin variables σ_i are the same value as both of

boundaries. The reason for these initial states is that these states are the most natural ground state which correspond to each of the boundary conditions.

All the simulations are performed by the single flip algorithm on the Metropolis probability. We performed these simulations for 480 samples for all parameters and averaged them, and then averaged along the time direction.

In addition, we also show their temperature derivatives to discuss the phase transitions.

4.1 Frictional Force Density $f(L_z, T)$

We show the behavior of the frictional force density $f(L_z, T)$ (see Figure 4.1). For both boundary conditions, the anti-parallel and the parallel, extremely smaller sizes such as $L_z = 4, 6$ make greater differences from its value for $L_z = 16$, where an asymptotic behavior emerges. We can expect that for more larger sizes such as $L_z = 18, 20, \dots$ makes no longer great differences from that of $L_z = 16$, thus we can say that the system reaches *two-dimension* in the vicinity of the size $L_z = 16$.

An additional important aspect is the difference between the values for anti-parallel and the parallel boundary conditions. In the former case, the smaller size L_z makes the greater value of the frictional force density $f(L_z, T)$. On the other hand, the latter case indicates the reverse behavior that smaller size L_z makes the smaller value of the frictional force density $f(L_z, T)$. This physical meaning is that the size L_z and the correlation length of the system along the z -direction $\xi_z(\beta)$ become comparable, and then the system behaves as one-dimensional one for the smaller size L_z , whereas much greater size L_z than the correlation length $\xi_z(\beta)$ makes the system two-dimensional. Note that for $L_z = 16$ behaviors for both cases are similar to each other and we can expect that these behaviors reach to the results by Kadau [2].

We additionally show the behavior of Its temperature derivative $\partial f(L_z, T)/\partial T$ (see Figure

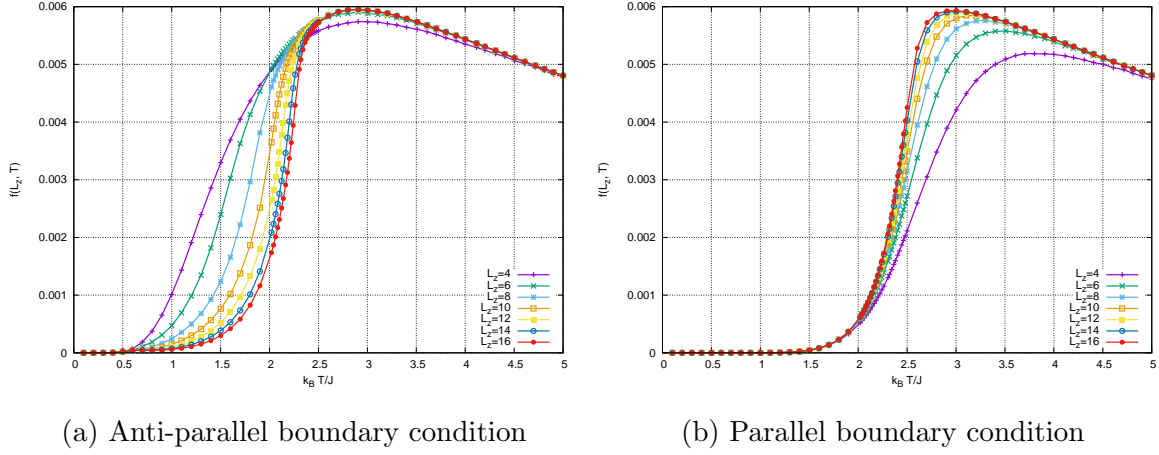
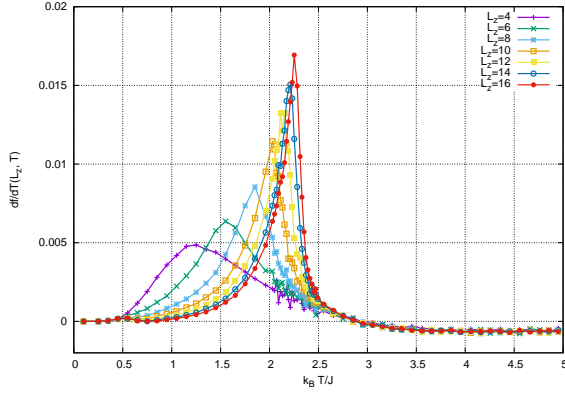


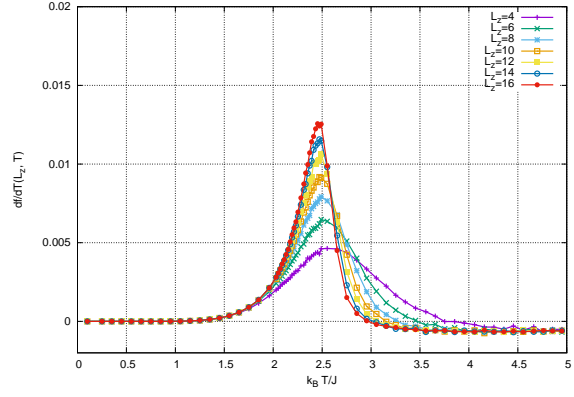
Figure 4.1: The temperature T dependence of the frictional force density $f(L_z, T)$ with the parallel boundary condition along the z -direction for each longitudinal size L_z are plotted.

4.2). These exhibits the crossover-driven divergence at characteristic temperatures, near $T = 2.25$ for the anti-parallel boundary and near $T = 2.50$ for the parallel boundary to reflect the steeper slopes of the frictional force density $f(L_z, T)$. If we regards the peak $T_{\text{peak}}(L_z)$ as the pseudo critical point for all sizes $L_z = 4, 6, 8, 10, 12, 14, 16$, where $\partial^2 f(L_z, T)/\partial T^2|_{T=T_{\text{peak}}(L_z)} = 0$, we can recognize the shift of peaks toward the higher temperature for the anti-parallel boundary, whereas peaks shifts toward the lower for the parallel boundary. These describes the effects of the boundary condition which acts on the system as an effective field, and the effects are enhanced by the smaller sizes L_z . Namely the anti-parallel boundary acts as a demagnetizing field such that the pseudo critical point $T_{\text{peak}}(L_z)$ shifts toward the lower, and the parallel boundary acts as a magnetizing field such that the pseudo critical point $T_{\text{peak}}(L_z)$ shifts toward the higher.

Remarkably peaks $T_{\text{peak}}(L_z)$ for both boundaries can be expected to hit the temperature higher than the ordinary critical point $T_c = \text{exact value or equation form}$. This implies that both the ordinary phase transition and the non-equilibrium phase transition occur at two different temperatures.



(a) Anti-parallel boundary condition



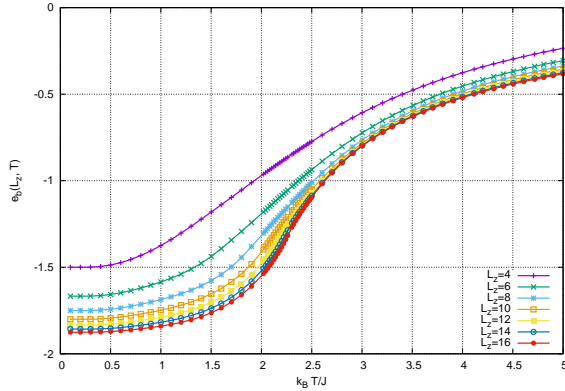
(b) Parallel boundary condition

Figure 4.2: The temperature T dependence of the temperature derivative $\partial f(L_z, T)/\partial T$ with the parallel boundary condition along the z -direction for each longitudinal size L_z are plotted.

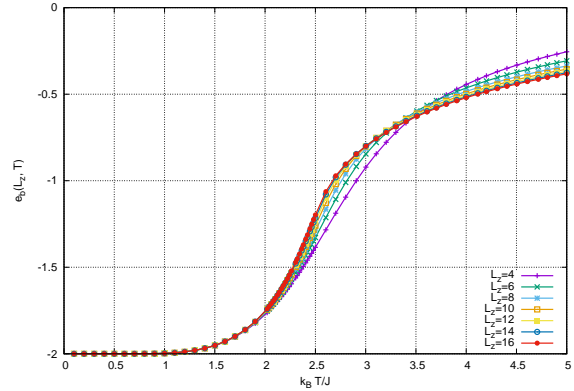
4.2 Bulk Energy Density $\epsilon_b(L_z, T)$

We show the behavior of the bulk energy density $\epsilon_b(L_z, T)$ (see Figure 4.3). As same as frictional force densities $f(L_z, T)$, bulk energy densities $\epsilon_b(L_z, T)$ indicates an asymptotic behavior.

In the anti-parallel case, the smaller size L_z makes the system well disorder. On the other hand, the parallel case indicates no drastic change driven by the smaller size L_z .



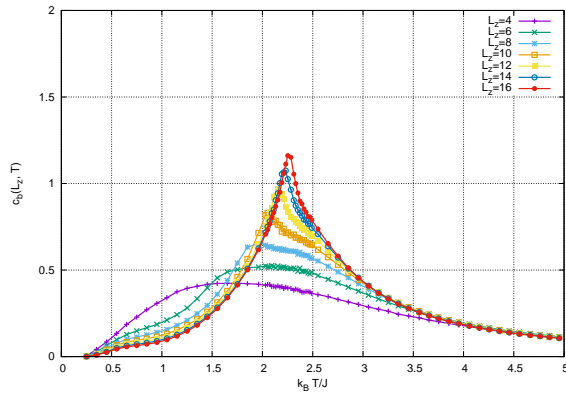
(a) Anti-parallel boundary condition



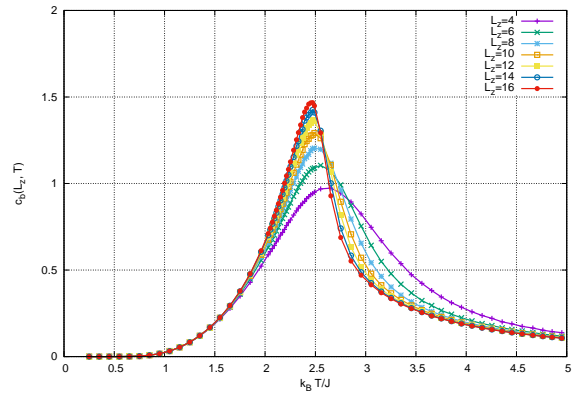
(b) Parallel boundary condition

Figure 4.3: The temperature T dependence of the bulk energy density $\epsilon_b(L_z, T)$ with the parallel boundary condition along the z -direction for each longitudinal size L_z are plotted.

We additionally show the behavior of Its temperature derivative $c_b(L_z, T) = \partial \epsilon_b(L_z, T)/\partial T$ (see Figure 4.2). The behavior is similar to that of the temperature derivative of the frictional force density $\partial f(L_z, T)/\partial T$ in terms of the peak $T_{\text{peak}}(L_z)$ for enough larger sizes.



(a) Anti-parallel boundary condition



(b) Parallel boundary condition

Figure 4.4: The temperature T dependence of the bulk energy density $\epsilon(L_z, T)$ with the parallel boundary condition along the z -direction for each longitudinal size L_z are plotted.

Chapter 5

Summary and Discussion

Summary.

Appendix A

Analysis based on Stochastic Matrices

In this chapter, we prove the existence of the non-equilibrium stationary state in our model with a half sliding for arbitrary velocities $v > 0$. In the first section, we discuss the formulation by stochastic matrices, and then see Monte Carlo simulations and the stochastic matrices are equivalent in terms of the probability with a simple example. In the following two sections, we prove several facts for stochastic matrices, which ensures that almost all Monte Carlo simulations converge to a equilibrium state and its uniqueness, and then the properties are taken over and lead to a unique stationary state even if the matrix contains a kind of perturbation factors. In the last two sections, we propose the way to construct the matrix for both equilibrium cases and non-equilibrium stationary cases, and discuss the distributions of their eigenvalues in terms of the convergence.

A.1 A Simple Example: Stochastic Ising Model with N -spins

Monte Carlo simulations for lattice spin systems extract the relevant subspace from the full space instead of an exact calculation of the partition function using a stochastic process. The subspace depends on given parameters and if we use the canonical distribution with a fixed temperature T , the temperature determines the subspace. The stochastic process is expressed as a trajectory of variables by the time in the subspace. Averaging the trajectory for an enough long time, we can compute physical quantities with any desired accuracy.

We now consider a matrix form of the stochastic process. For example, the one-dimensional Ising chain with N -spins has 2^N states. If we labeled each of the states by $i = 1, 2, \dots, 2^N$, we can write the stochastic time evolution of the system by a set of the existence probabilities $\{p_i(t)\}$ such that the system is in the i -th state at a time t , and the transition probabilities T_{ij} such that the system in the j -th state changes to the i -th state. Note that not the transition probabilities T_{ij} but the existence probabilities $\{p_i(t)\}$ play the role of time evolution.

We additionally define the conditional probability $\tilde{p}_{ij}(t)$ such that the system in the j -th state at a time t changes to the i -th state at the next time $t + 1$. Using the conditional probability, we can derive the relation between the existence probability $p_i(t)$ and the transition probability T_{ij} as

$$\tilde{p}_{ij}(t + 1) = T_{ij}p_j(t) \quad \text{for } 1 \leq i, j \leq 2^N. \quad (\text{A.1})$$

From a property as the probability, it should hold that $\sum_{i=1}^{2^N} p_i(t) = 1$ and $p_i(t) \geq 0$ ($i = 1, 2, \dots, 2^N, t \in \mathbb{R}$). The conditional probability $\tilde{p}_{ij}(t)$ should also satisfy the condition that

$\sum_{j=1}^{2^N} \tilde{p}_{ij}(t) = p_i(t+1)$ ($i = 1, 2, \dots, 2^N, t \in \mathbb{R}$). Then we have

$$p_i(t+1) = \sum_{j=1}^{2^N} \tilde{p}_{ij}(t+1) = \sum_{j=1}^{2^N} T_{ij} p_j(t) \quad \text{for } 1 \leq i \leq 2^N, t \in \mathbb{R}. \quad (\text{A.2})$$

In the other words, the system can be described by the probability vector $\mathbf{p}(t) := {}^t(p_1(t), p_2(t), \dots, p_{2^N}(t))$ and the stochastic matrix $\hat{T} := (T_{ij})$ as

$$\mathbf{p}(t+1) = \hat{T}\mathbf{p}(t) \quad \text{for } t \in \mathbb{R}. \quad (\text{A.3})$$

In Monte Carlo simulations, we often trace the trajectory of a component of the vector $\mathbf{p}(t)$, thus we rarely need to construct the matrix \hat{T} . But it is helpful for us to consider such the matrix when we discuss the convergence to the stationary state or its uniqueness. These discussions are valid for general Ω -dimensional state spaces, thus we denote the number of states by Ω from now on.

A.2 General Theory of Stochastic Matrices

In this section we discuss the conditions which ensure a convergence of the corresponding Monte Carlo simulation to a unique stationary state. We first define the stochastic matrix and discuss fundamental properties of the stochastic matrix. We next discuss the properties which result from an additional condition called *weak/strong connectivity*, which leads the existence and the uniqueness of a stationary state. We also see that we can construct a stochastic matrix which leads to any desired stationary state under the so-called *detailed balanced condition*.

From the condition $\sum_{i=1}^{\Omega} p_i(t) = 1$ and $p_i(t) \geq 0$ ($i = 1, 2, \dots, \Omega, t \in \mathbb{R}$), we have a set of properties $\sum_{i=1}^{\Omega} T_{ij} = 1$, $T_{ij} \geq 0$ ($1 \leq i \leq \Omega$). Any matrix with these conditions is called

stochastic matrix and shows the following interesting property:

Theorem A.2.1. Let \hat{T} be a stochastic matrix, then all absolute values of eigenvalue are less than or equal to 1. For any eigenvector $\mathbf{x} = {}^t\{x_1, x_2, \dots, x_\Omega\}$ which does *not* belong to the eigenvalue 1, it additionally holds that

$$\sum_{j=1}^{\Omega} x_j = 0. \quad (\text{A.4})$$

We now define the vector $\mathbf{d} := {}^t(1, 1, \dots, 1)$ to prove all facts after this.

Proof. For any stochastic matrix \hat{T} , we have

$$\left({}^t\hat{T}\mathbf{d}\right)_i = \sum_{j=1}^N ({}^tT)_{ij} d_j = \sum_{j=1}^N T_{ji} d_j = \sum_{j=1}^N T_{ji} = 1 \quad \text{for } i = 1, 2, \dots, N, \quad (\text{A.5})$$

$$\iff {}^t\hat{T}\mathbf{d} = \mathbf{d}. \quad (\text{A.6})$$

Therefore the matrix ${}^t\hat{T}$ has an eigenvalue 1 at least. The eigenequation for the matrix ${}^t\hat{T}$ are rewritten as

$$\det \left[\lambda \hat{I}_N - {}^t\hat{T} \right] = \det \left[{}^t \left(\lambda \hat{I}_N - \hat{T} \right) \right] = \det \left[\lambda \hat{I}_N - \hat{T} \right], \quad (\text{A.7})$$

and then the set of eigenvalues of \hat{T} is equal to that of ${}^t\hat{T}$. Finally the matrix \hat{T} has an eigenvalue 1 at least. A general eigenvalue equation of \hat{T} can be written as

$$\hat{T}\mathbf{x}_\lambda = \lambda \mathbf{x}_\lambda, \quad (\text{A.8})$$

where $\mathbf{x}_\lambda = {}^t(x_{\lambda,1}, x_{\lambda,2}, \dots, x_{\lambda,N})$ is its eigenvector. We have

$$((l.h.s \text{ of A.8}), \mathbf{d}) = (\hat{T}\mathbf{x}_\lambda, \mathbf{d}) = (\mathbf{x}_\lambda, {}^t\hat{T}\mathbf{d}) = (\mathbf{x}_\lambda, \mathbf{d}), \quad (\text{A.9})$$

$$((r.h.s \text{ of A.8}), \mathbf{d}) = (\lambda\mathbf{x}_\lambda, \mathbf{d}) = \lambda(\mathbf{x}_\lambda, \mathbf{d}). \quad (\text{A.10})$$

$$\iff (1 - \lambda)(\mathbf{x}_\lambda, \mathbf{d}) = 0 \iff \lambda = 1 \text{ or } (\mathbf{x}_\lambda, \mathbf{d}) = 0. \quad (\text{A.11})$$

$$\iff \sum_{i=1}^N x_{\lambda,i} = 0 \quad \text{if } \lambda \neq 1. \quad (\text{A.12})$$

We additionally define the vector $\mathbf{y}_\lambda := {}^t(|x_{\lambda,1}|, |x_{\lambda,2}|, \dots, |x_{\lambda,N}|)$ for any λ . From the equation

$\sum_{j=1}^N T_{ij}x_{\lambda,j} = \lambda x_i$ ($i = 1, 2, \dots, N$) we have

$$\left| \sum_{j=1}^N T_{ij}x_{\lambda,j} \right| \leq \sum_{j=1}^N T_{ij}|x_{\lambda,j}| \quad (\because T_{ij} \geq 0 \text{ for } j = 1, 2, \dots, N) \quad (\text{A.13})$$

$$= \left(\hat{T}\mathbf{y}_\lambda \right)_i \quad \text{for } i = 1, 2, \dots, N. \quad (\text{A.14})$$

and the left hand side of (A.14) are rewritten as

$$\left| \sum_{j=1}^N T_{ij}x_{\lambda,j} \right| = |\lambda x_{\lambda,i}| = |\lambda| \times |x_{\lambda,i}| = |\lambda| \times (\mathbf{y}_\lambda)_i, \quad (\text{A.15})$$

thus we have

$$|\lambda| \times (\mathbf{y}_\lambda)_i \leq \left(\hat{T}\mathbf{y}_\lambda \right)_i, \quad (\text{A.16})$$

$$\iff |\lambda| \times (\mathbf{y}_\lambda, \mathbf{d}) \leq \left(\hat{T}\mathbf{y}_\lambda, \mathbf{d} \right) = \left(\mathbf{y}_\lambda, {}^t\hat{T}\mathbf{d} \right) = (\mathbf{y}_\lambda, \mathbf{d}), \quad (\text{A.17})$$

$$\iff |\lambda| \leq 1. \quad (\text{A.18})$$

□

We limit the class of stochastic matrices to that of weakly connected ones from now on.

Definition A.2.1. For an arbitrary $1 \leq i, j \leq N$, if there exists an $n(i, j) > 0$ such that

$$\left(\hat{T}^{n(i,j)}\right)_{ij} > 0, \quad (\text{A.19})$$

the matrix \hat{T} is called *weakly connected*. Note that for any $n' > n(i, j)$ it does *not* follow that $\left(\hat{T}^{n'}\right)_{ij} > 0$.

To make proofs easier, we also define the matrix $\hat{\mathcal{T}}_\epsilon$ ($\epsilon > 0$) and discuss its properties.

Denoting the maximum value of $n(i, j)$ by $n_{\max} := \max_{1 \leq i, j \leq N} [n(i, j)]$ and defining the matrix

$\hat{\mathcal{T}}_\epsilon := \left(\hat{I}_N + \epsilon \hat{T}\right)^{n_{\max}}$, we have

$$\left(\hat{\mathcal{T}}_\epsilon\right)_{ij} = \left(\left(\hat{I}_N + \epsilon \hat{T}\right)^{n_{\max}}\right)_{ij} = \sum_{k=1}^{n_{\max}} \binom{n_{\max}}{k} \left(\hat{I}_N^k \left(\epsilon \hat{T}\right)^{n_{\max}-k}\right)_{ij} \quad (\text{A.20})$$

$$= \sum_{k=1}^{n_{\max}} \binom{n_{\max}}{k} \epsilon^{n_{\max}-k} \left(\hat{T}^{n_{\max}-k}\right)_{ij} \geq 0 \quad (\because T_{ij} > 0) \quad \text{for } 1 \leq i, j \leq N. \quad (\text{A.21})$$

For the eigenvector $\mathbf{x}_1 = {}^t(x_{1,1}, x_{1,2}, \dots, x_{1,N})$, which belongs to the eigenvalue 1, it holds that

$$\hat{\mathcal{T}}_\epsilon \mathbf{x}_1 = \sum_{k=1}^{n_{\max}} \binom{k}{n_{\max}} \epsilon^{n_{\max}-k} \hat{T}^{n_{\max}-k} \mathbf{x}_1 \quad (\text{A.22})$$

$$= \sum_{k=1}^{n_{\max}} \binom{k}{n_{\max}} \epsilon^{n_{\max}-k} \mathbf{x}_1 \quad (\text{A.23})$$

$$= (1 + \epsilon)^{n_{\max}} \mathbf{x}_1, \quad (\text{A.24})$$

and each component is

$$\sum_{j=1}^N \left(\hat{\mathcal{T}}_{\epsilon} \right)_{ij} x_{1,j} = (1 + \epsilon)^{n_{\max}} x_{1,i} \quad \text{for } i = 1, 2, \dots, N. \quad (\text{A.25})$$

Theorem A.2.2. The phases of components of the vector \mathbf{x}_1 are aligned together and all the components are positive. In other words, we can decompose the vector into a phase factor and a positive vector as follows

$$\mathbf{x}_1 = e^{i\theta} \mathbf{u}_1, \quad (\text{A.26})$$

where θ is the phase and \mathbf{u}_1 is the vector with all positive component.

Proof. If components of the vector \mathbf{x}_1 are *not* aligned together such that $\sum_{i=1}^N |x_{1,i}| > |\sum_{i=1}^N x_{1,i}|$ holds, we have

$$\left| \sum_{j=1}^N \left(\hat{\mathcal{T}}_{\epsilon} \right)_{ij} x_{1,j} \right| < \sum_{j=1}^N \left(\hat{\mathcal{T}}_{\epsilon} \right)_{ij} |x_{1,j}| = (1 + \epsilon)^{n_{\max}} |x_{1,i}|. \quad (\text{A.27})$$

On the other hand, the row-wise sum of the matrix $\hat{\mathcal{T}}_{\epsilon}$ are

$$\sum_{i=1}^N \left(\hat{\mathcal{T}}_{\epsilon} \right)_{ij} = \sum_{k=1}^{n_{\max}} \binom{k}{n_{\max}} \epsilon^{n_{\max}-k} \sum_{i=1}^N \left(\hat{\mathcal{T}}^{n_{\max}-k} \right)_{ij} = (1 + \epsilon)^{n_{\max}}. \quad (\text{A.28})$$

Then we have

$$\sum_{i=1}^N \sum_{j=1}^N \left(\hat{\mathcal{T}}_{\epsilon} \right)_{ij} |x_{1,j}| = (1 + \epsilon)^{n_{\max}} \sum_{j=1}^N |x_{1,j}| > (1 + \epsilon)^{n_{\max}} \sum_{i=1}^N |x_{1,i}|, \quad (\text{A.29})$$

but it is the contradiction caused from our assumption $\sum_{i=1}^N |x_{1,i}| > |\sum_{i=1}^N x_{1,i}|$. Furthermore the left hand side of (A.25) is positive because that n_{\max} is the maximum value of $n(i, j)$, and

then the right hand side is also positive. Then we have $x_{1,i} > 0 (i = 1, 2, \dots, N)$. \square

Theorem A.2.3. The eigenspace of the matrix $\hat{\mathcal{T}}_\epsilon$, which belongs to the eigenvalue 1, is *one-dimensional*.

Proof. If we have two different eigenvectors, which belongs to the eigenvalue 1, we can write their eigenequations by two different *positive vectors* as

$$\hat{T}\mathbf{u}_1 = \mathbf{u}_1, \tag{A.30}$$

$$\hat{T}\mathbf{v}_1 = \mathbf{v}_1. \tag{A.31}$$

For their any linear superposition, we also have

$$\hat{T}(\mathbf{u}_1 + t\mathbf{v}_1) = \mathbf{u}_1 + t\mathbf{v}_1, \quad \text{for any } t \in \mathbb{R}. \tag{A.32}$$

But if two eigenvectors \mathbf{u}_1 and \mathbf{v}_1 are not aligned, we can make a non-trivial vector with a certain t such that $(\mathbf{u}_1 + t\mathbf{v}_1)_l = 0$ for an l -th element. But it is the contradiction with the fact $x_{1,i} > 0 (i = 1, 2, \dots, N)$. Then we have no eigenspaces more than one, which belongs to the eigenvalue 1. \square

We additionally limit the class of stochastic matrices to that of strongly connected ones from now on.

Definition A.2.2. If there exists a number $N_0 > 0$ such that

$$\left(\hat{T}^{N_0}\right)_{ij} > 0 \tag{A.33}$$

for an arbitrary $1 \leq i, j \leq N$, the matrix \hat{T} is called *strongly connected*.

Theorem A.2.4. There exists only the eigenvalue 1 with its absolute value 1.

Proof. We now have $\hat{T}^n \mathbf{u}_\lambda = \lambda^n \mathbf{u}_\lambda$, where $\mathbf{u}_\lambda = {}^t(u_{\lambda,1}, u_{\lambda,2}, \dots, u_{\lambda,N})$ is the eigenvector which belongs to an eigenvalue λ . Their components are written as

$$\sum_{j=1}^N \left(\hat{T}^n \right)_{ij} u_{\lambda,j} = \lambda^n u_{\lambda,i}, \quad \text{for } i = 1, 2, \dots, N. \quad (\text{A.34})$$

We can divide conditions for λ into following two cases:

Case1: $\sum_{i=1}^N |u_{\lambda,i}| > |\sum_{i=1}^N u_{\lambda,i}|$,

We have

$$\sum_{j=1}^N \left(\hat{T}^n \right)_{ij} |u_{\lambda,j}| > \left| \sum_{j=1}^N \left(\hat{T}^n \right)_{ij} u_{\lambda,j} \right| = |\lambda^n| \times |u_{\lambda,i}|, \quad \text{for } i = 1, 2, \dots, N. \quad (\text{A.35})$$

$$\iff |\lambda^n| < 1 \iff |\lambda| < 1. \quad (\text{A.36})$$

Case2: $\sum_{i=1}^N |u_{\lambda,i}| = |\sum_{i=1}^N u_{\lambda,i}|$.

We have

$$\sum_{i=1}^N \sum_{j=1}^N \left(\hat{T}^n \right)_{ij} u_{\lambda,j} = \sum_{j=1}^N u_{\lambda,j} = \lambda^n \sum_{i=1}^N u_{\lambda,i}. \quad (\text{A.37})$$

$$\iff \lambda^n = 1 \quad (\because \mathbf{u}_\lambda \neq \mathbf{0}, u_{\lambda,i} \geq 0 \Rightarrow \sum_{i=1}^N u_{\lambda,i} > 0). \quad (\text{A.38})$$

Thus there is only an eigenvalue 1 with its absolute value 1. □

Theorem A.2.5. The vector $\lim_{N \rightarrow \infty} \hat{T}^N \mathbf{r} = \mathbf{0}$ for any $\mathbf{r} \in \mathbb{C}$ is orthogonal to \mathbf{d} .

Proof. For an arbitrary vector \mathbf{r} , we can decompose it into its real and imaginary parts as

$\mathbf{r} = \mathbf{r}_R + i\mathbf{r}_I$. Since the condition $(\mathbf{r}, \mathbf{d}) = 0$ is equivalent to $\sum_{i=1}^N r_i = 0$, we have

$$\sum_{j \in I_+} r_j + \sum_{j \in I_-} r_j = 0, \quad (\text{A.39})$$

where $I_{\pm} := \{j \mid r_j \gtrless 0, 1 \leq j \leq N\}$. Note that $\sum_{j \in I_+} r_j = \sum_{j \in I_-} |r_j|$. Thus we have

$$\sum_{j \in I_+} r_j = \sum_{j \in I_-} |r_j| = \|\mathbf{r}\|_1/2. \quad (\text{A.40})$$

Since \hat{T} is strongly connected, there is an integer N_0 such that $(\hat{T}^{N_0})_{ij} > 0$ for an arbitrary

$1 \leq i, j \leq N$. For the N_0 we have

$$(\hat{T}^{N_0} \mathbf{r}) = \sum_{j=1}^N (\hat{T}^{N_0})_{ij} r_j = \sum_{j \in I_+} (\hat{T}^{N_0})_{ij} r_j - \sum_{j \in I_-} (\hat{T}^{N_0})_{ij} |r_j| \quad (\text{A.41})$$

$$= \sum_{j=1}^N (\hat{T}^{N_0})_{ij} r_j - 2 \sum_{j \in I_-} (\hat{T}^{N_0})_{ij} |r_j| \quad (\text{A.42})$$

$$\leq \sum_{j=1}^N (\hat{T}^{N_0})_{ij} r_j - 2\delta_{N_0} \sum_{j \in I_-} |r_j| \quad (\text{A.43})$$

$$= \sum_{j=1}^N (\hat{T}^{N_0})_{ij} r_j - \delta_{N_0} \|\mathbf{r}\|_1, \quad (\text{A.44})$$

where $\delta_{N_0} := \min_{1 \leq i, j \leq N} \left[(\hat{T}^{N_0})_{ij} \right]$ (for $i = 1, 2, \dots, N$). Note that there exists a $\delta_{N_0} > 0$ for the

strongly connected matrix \hat{T} . Similarly we have

$$\left(\hat{T}^{N_0}\mathbf{r}\right) = \sum_{j=1}^N \left(\hat{T}^{N_0}\right)_{ij} r_j = \sum_{j \in I_+} \left(\hat{T}^{N_0}\right)_{ij} r_j - \sum_{j \in I_-} \left(\hat{T}^{N_0}\right)_{ij} |r_j| \quad (\text{A.45})$$

$$= 2 \sum_{j \in I_+} \left(\hat{T}^{N_0}\right)_{ij} r_j - \sum_{j=1}^N \left(\hat{T}^{N_0}\right)_{ij} |r_j| \quad (\text{A.46})$$

$$\geq 2\delta_{N_0} \sum_{j \in I_+} r_j - \sum_{j=1}^N \left(\hat{T}^{N_0}\right)_{ij} |r_j| \quad (\text{A.47})$$

$$= \delta_{N_0} \|\mathbf{r}\|_1 - \sum_{j=1}^N \left(\hat{T}^{N_0}\right)_{ij} |r_j|, \quad (\text{for } i = 1, 2, \dots, N). \quad (\text{A.48})$$

Combining them, we have

$$|\left(\hat{T}^{N_0}\mathbf{r}\right)| \leq \sum_{j=1}^N \left(\hat{T}^{N_0}\right)_{ij} |r_j| - \delta_{N_0} \|\mathbf{r}\|_1, \quad (\text{for } i = 1, 2, \dots, N), \quad (\text{A.49})$$

and then it holds that

$$\|\hat{T}^{N_0}\mathbf{r}\|_1 = \sum_{i=1}^N |\left(\hat{T}^{N_0}\mathbf{r}\right)_i| \leq \sum_{j=1}^N |r_j| - N_0 \delta_{N_0} \|\mathbf{r}\|_1 = (1 - N\delta_{N_0}) \|\mathbf{r}\|_1. \quad (\text{A.50})$$

The vector $\hat{T}^{N_0}\mathbf{r}$ is also orthogonal to the vector \mathbf{d} , actually it holds that

$$\left(\hat{T}^{N_0}\mathbf{r}, \mathbf{d}\right) = \left(\mathbf{r}, {}^t\left(\hat{T}^{N_0}\right)\mathbf{d}\right) = \left(\mathbf{r}, \left({}^t\hat{T}\right)^{N_0}\mathbf{d}\right) = (\mathbf{r}, \mathbf{d}) = 0. \quad (\text{A.51})$$

Then, for any positive integer l , we can repeat this discussion as

$$\|\hat{T}^{N_0 l}\mathbf{r}\|_1 \leq (1 - N_0 \delta_{N_0})^l \|\mathbf{r}\|_1. \quad (\text{A.52})$$

Since $N_0 > 0$, $\delta_{N_0} > 0$ and thus $1 - N_0\delta_{N_0} < 0$, we have

$$\lim_{l \rightarrow \infty} (1 - N_0\delta_{N_0})^l \|\mathbf{r}\|_1 = 0. \quad (\text{A.53})$$

$$\iff \lim_{l \rightarrow \infty} \|\hat{T}^{N_0 l} \mathbf{r}\|_1 = 0. \quad (\text{A.54})$$

Thus, for an arbitrary positive integer N , we have

$$\lim_{N \rightarrow \infty} \|\hat{T}^N \mathbf{r}\|_1 = 0. \quad (\text{A.55})$$

□

Theorem A.2.6. We can write any vector \mathbf{x} as the superposition of \mathbf{u}_1 and \mathbf{r} .

Proof. Defining the coefficient $c_{1,\mathbf{x}} := (\mathbf{x}, \mathbf{d})/(\mathbf{u}_1, \mathbf{d})$ and the vector $\mathbf{r}_{\mathbf{x}} := \mathbf{x} - c_{1,\mathbf{x}}\mathbf{u}_1$, we have

$$(\mathbf{r}_{\mathbf{x}}, \mathbf{d}) = (\mathbf{x}, \mathbf{d}) - \frac{(\mathbf{x}, \mathbf{d})}{(\mathbf{u}_1, \mathbf{d})}(\mathbf{u}_1, \mathbf{d}) = 0, \quad (\text{A.56})$$

$$\mathbf{x} = c_{1,\mathbf{x}}(\mathbf{u}_1, \mathbf{d}) + \mathbf{r}_{\mathbf{x}}. \quad (\text{A.57})$$

□

Theorem A.2.7. The limit $\lim_{N \rightarrow \infty} \hat{T}^N \mathbf{p}^{(0)}$ is independent on the initial vector $\mathbf{p}^{(0)}$ and it holds that

$$\lim_{N \rightarrow \infty} \hat{T}^N \mathbf{p}^{(0)} = \frac{\mathbf{u}_1}{\|\mathbf{u}_1\|_1}, \quad (\text{A.58})$$

where the vector $\mathbf{p}^{(0)} = {}^t \{p_1^{(0)}, p_2^{(0)}, \dots, p_\Omega^{(0)}\}$ is in the class of probability vectors and then it is normalized $\sum_{i=1}^{\Omega} p_i^{(0)} = 1$.

Proof. From the theorem A.2.6, we have

$$\hat{T}^N \mathbf{p}^{(0)} = c_{1,\mathbf{p}^{(0)}} \hat{T}^N \mathbf{u}_1 + \hat{T}^N \mathbf{r}_{\mathbf{p}^{(0)}} = c_{1,\mathbf{p}^{(0)}} \mathbf{u}_1 + \hat{T}^N \mathbf{r}_{\mathbf{p}^{(0)}}. \quad (\text{A.59})$$

Its limit $N \rightarrow \infty$ is taken as

$$\lim_{N \rightarrow \infty} \hat{T}^N \mathbf{p}^{(0)} = c_{1,\mathbf{p}^{(0)}} \mathbf{u}_1 + \lim_{N \rightarrow \infty} \hat{T}^N \mathbf{r}_{\mathbf{p}^{(0)}} = c_{1,\mathbf{p}^{(0)}} \mathbf{u}_1. \quad (\text{A.60})$$

Using the matrix $\hat{A} := \mathbf{u}_1^t \mathbf{d} / (\mathbf{u}_1, \mathbf{d})$, we have

$$\left(\hat{A} \mathbf{p}^{(0)} \right)_i = \sum_{j=1}^N \frac{(\mathbf{u}_1)_i}{(\mathbf{u}_1, \mathbf{d})} (\mathbf{p}^{(0)})_j = (\mathbf{p}^{(0)}, \mathbf{d}) \frac{(\mathbf{u}_1)_i}{(\mathbf{u}_1, \mathbf{d})}, \quad \text{for } i = 1, 2, \dots, N. \quad (\text{A.61})$$

Then it leads

$$\hat{A} \mathbf{p}^{(0)} = \frac{(\mathbf{u}_1)_i}{(\mathbf{u}_1, \mathbf{d})} \mathbf{p}^{(0)} = c_{1,\mathbf{p}^{(0)}} \mathbf{p}^{(0)}. \quad (\text{A.62})$$

Then the limit $N \rightarrow \infty$ for $\hat{T}^N \mathbf{p}^{(0)}$ is rewritten by a simple multiplication as follows

$$\lim_{N \rightarrow \infty} \hat{T}^N \mathbf{p}^{(0)} = \frac{\mathbf{u}_1^t \mathbf{d}}{(\mathbf{u}_1, \mathbf{d})} \mathbf{p}^{(0)}. \quad (\text{A.63})$$

The expression (A.63) lead to the relation $\lim_{N \rightarrow \infty} \hat{T}^N \mathbf{p}^{(0)} = \mathbf{u}_1 / \|\mathbf{u}_1\|_1$. Actually it holds that

$$\frac{\mathbf{u}_1^t \mathbf{d}}{(\mathbf{u}_1, \mathbf{d})} (\mathbf{p}^{(0)})_i = \frac{\sum_{j=1}^N (\mathbf{u}_1)_i (\mathbf{d})_j (\mathbf{p}^{(0)})_j}{(\mathbf{u}_1, \mathbf{d})} = \frac{u_{1,i}}{\|\mathbf{u}_1\|_1}, \quad (\text{A.64})$$

thus we have

$$\lim_{N \rightarrow \infty} \hat{T}^N \mathbf{p}^{(0)} = \frac{\mathbf{u}_1}{\|\mathbf{u}_1\|_1}. \quad (\text{A.65})$$

□

Once we get a strongly connected stochastic matrix \hat{T} , its stationary distribution $\mathbf{u}_1/\|\mathbf{u}_1\|_1$ is determined independently on the initial distribution. We can consider this procedure as a *transformation* from the matrix \hat{T} into the vector $\mathbf{u}_1/\|\mathbf{u}_1\|_1$.

On the other hand, we can also consider the inverse transformation. This means the *construction* of the matrix \hat{T}' with a *desired* stationary distribution \mathbf{p}' . We can actually formulate such the procedure using the *detailed balanced condition* as follows.

Detailed Balanced Condition

If a vector $\mathbf{p}' = {}^t(p'_1, p'_2, \dots, p'_\Omega)$ is the stationary distribution of the stochastic matrix $\hat{T}' = (T'_{ij})$, it holds that

$$T'_{ij}p'_j = T'_{ji}p'_i \quad (\text{A.66})$$

for $1 \leq i, j \leq \Omega$.

This property is simplified by summing over the subscription i as follows

$$\sum_{i=1}^{\Omega} T'_{ij}p'_j = p'_j = \sum_{i=1}^{\Omega} T'_{ji}p'_i = \left(\hat{T}\mathbf{p}'\right)_j, \quad \text{for } j = 1, 2, \dots, \Omega. \quad (\text{A.67})$$

Then if the detailed balanced condition holds for a matrix \hat{T}' , the corresponding vector \mathbf{p}' is the fixed point of the matrix \hat{T}' . Thus in order to get the matrix \hat{T}' which lead any distribution $\mathbf{p}^{(0)}$ to the desired distribution \mathbf{p}' , we only have to construct each element T'_{ij} of the matrix

according to the condition (A.66) and make the matrix strongly connected.

In Monte Carlo simulations of statistical mechanics, we calculate the equilibrium distribution $\mathbf{p}_{\text{eq}}(\beta)$ at an inverse temperature β using an initial state i_0 and a rule of the stochastic process $i \rightarrow j \rightarrow j' \rightarrow \dots$. We can regard the matrix construction method as a set of the stochastic process $i_0 \rightarrow j \rightarrow j' \rightarrow \dots$ over all possible states $i_0 = 1, 2, \dots, \Omega$. In other words, the matrix T_{ij} corresponding to a simulation contains the information of all possible initial states $i_0 = 1, 2, \dots, \Omega$ and all possible transitions $T_{1,i_0}, T_{2,i_0}, \dots, T_{\Omega,i_0}$ respectively from them. Thus we often consider a *sample path* by an appropriate initial state and the matrix.

The condition (A.66) or

$$\frac{T_{ij}}{T_{ji}} = \frac{p_i}{p_j} \quad (\text{A.68})$$

is not sufficient to determine a concrete form of the matrix \hat{T} and thus in general there is a degree of freedom in the form of \hat{T} . For Monte Carlo simulations of equilibrium statistical mechanics, this freedom also remains as follows:

$$\frac{T_{ij}(\beta)}{T_{ji}(\beta)} = \frac{p_i(\beta)}{p_j(\beta)} = e^{-\beta(E_i - E_j)}, \quad \text{for } 1 \leq i, j \leq N, \quad (\text{A.69})$$

where $T_{ij}(\beta)$ and $p_i(\beta)$ are the matrix corresponding to a simulation and the probability that the i -th state emerges respectively with a fixed inverse temperature β . But this relation is important that the rate of transition probabilities is always given by a difference of energy eigenvalues $\{E_1, E_2, \dots, E_\Omega\}$, and thus we do *not* have to calculate exact values of $\tilde{p}_i(\beta) := \exp[-\beta E_i] / Z(\beta)$ ($Z(\beta) := \sum_i \exp[-\beta E_i]$).

If we use the Metropolis probability for the N -spins system, each element of the matrix

$(T_{ij}(\beta))$ is written as follows.

$$T_{ij}(\beta) = \begin{cases} \frac{1}{N} \min [1, e^{-\beta(E_i - E_j)}] & \text{for states } i, j \text{ mutually reachable by a single flip,} \\ 0 & \text{for states } i, j \text{ not mutually reachable by a single flip.} \end{cases} \quad (\text{A.70})$$

The factor $1/N$ describes the equivalent selection of a spin to flip.

A.2.1 Construction of the Stochastic Matrix based on the Detailed Balanced Condition

Cite the mathematica results.

A.3 Stochastic Matrices and Non-Equilibrium Monte Carlo Simulations

A.4 Calculation Non-Equilibrium Observables by the Stochastic Matrices

Appendix B

Results of Simulations in More Detail

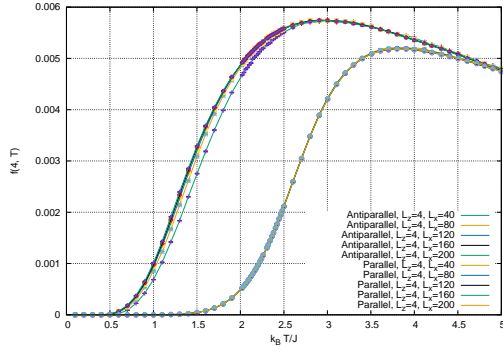
B.1 Checking the Convergence in the Limit $L_x \rightarrow \infty$

We now demonstrate that following two observables are converging at corresponding numerical large size limits.

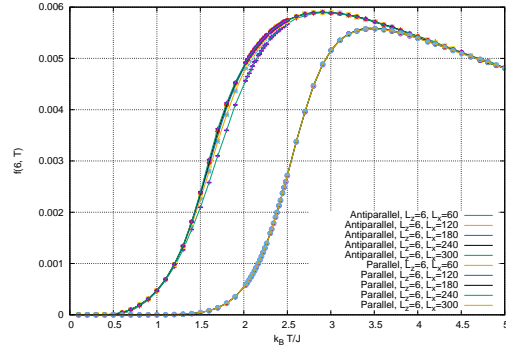
$$f(L_z, T) := \lim_{L_x \rightarrow \infty} \frac{F(L_x, L_z, T)}{L_x} \quad (\text{B.1})$$

$$\epsilon_b(L_z, T) := \lim_{L_x \rightarrow \infty} \frac{E_b(L_x, L_z, T)}{L_x L_z} \quad (\text{B.2})$$

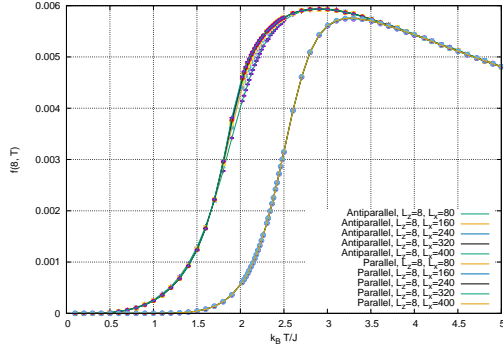
Both of them have no dependence on L_x and also do not diverge in the limit of L_z . Thus we can analyze these qualitative and pure dependence on L_z and T . We use the aspect of $L_x = 10L_z, 20L_z, \dots, 50L_z$ for checking the convergence in the limit $L_x/L_z \rightarrow \infty$ with fixed L_z .



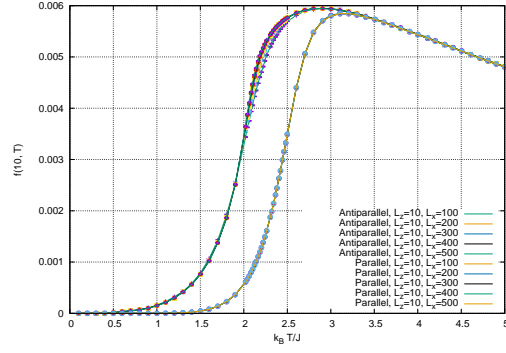
(a) $L_z = 4$



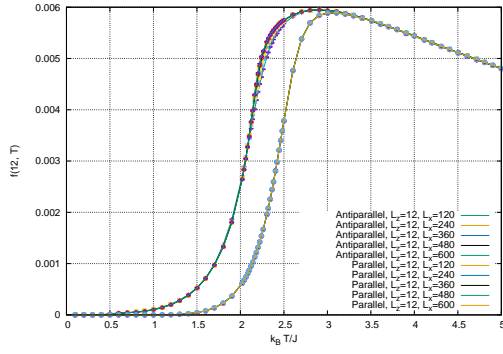
(b) $L_z = 6$



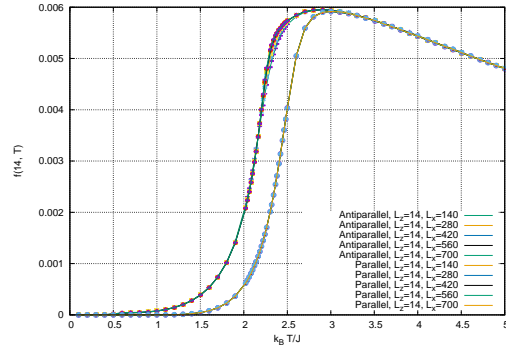
(c) $L_z = 8$



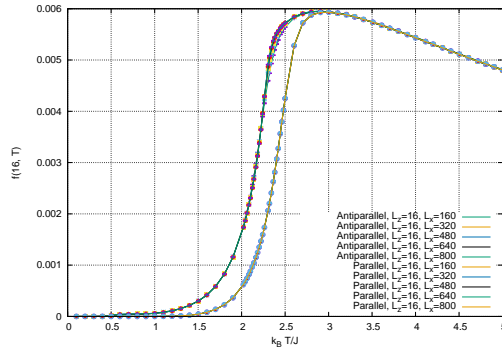
(d) $L_z = 10$



(e) $L_z = 12$



(f) $L_z = 14$



(g) $L_z = 16$

Figure B.1: Each data shows $F(L_x, L_z, T)/L_x$ versus T .

B.1.1 Dependence of $F(L_x, L_z, T)/L_x$ on L_x for each L_z

We show that the quantity $F(L_x, L_z, T)/L_x$ has no dependence on L_x at a sufficient large L_x for each L_z . The following graphs are the temperature dependence of the frictional force density with each of boundary conditions along the z -direction for each of longitudinal size $L_z = 4, 6, 8, 10, 12, 14, 16$ (fig.B.1).

B.1.2 Dependence of $E_b(L_x, L_z, T)/(L_x L_z)$ on L_x for each L_z

We show that the quantity $E_b(L_x, L_z, T)/L_x$ has no dependence on L_x at a sufficient large L_x for each L_z . The following graphs are the temperature dependence of the frictional force density with each of boundary conditions along the z -direction for each of longitudinal size $L_z = 4, 6, 8, 10, 12, 14, 16$ (fig.B.2).

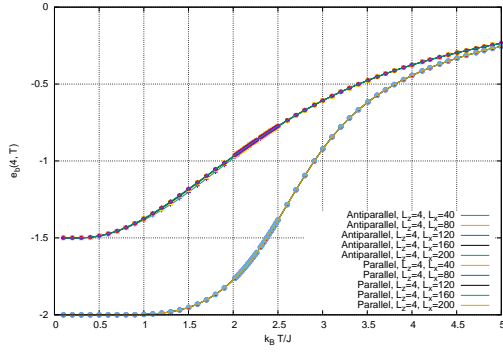
B.2 Time Series of Observables

We now show the data which we use to calculate the long time limit of power $P(t)$, dissipation rate $D(t)$ and bulk energy $E_b(t)$.

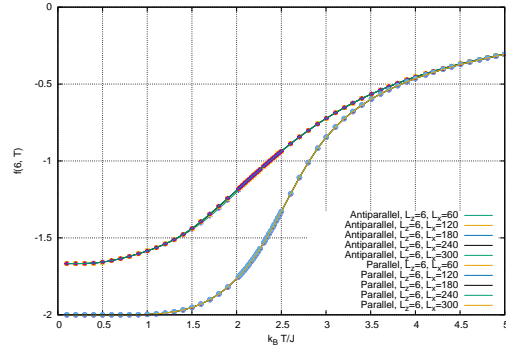
We can estimate the non-equilibrium correlation time of these observables, and then the valid interval in each time series are determined.

B.2.1 title

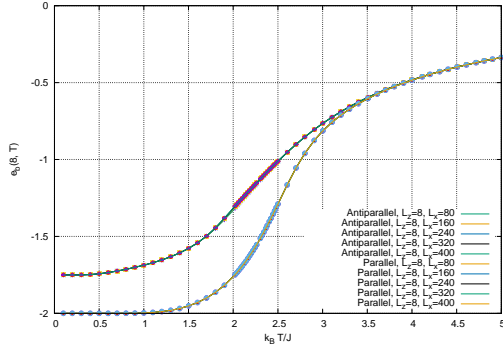
title



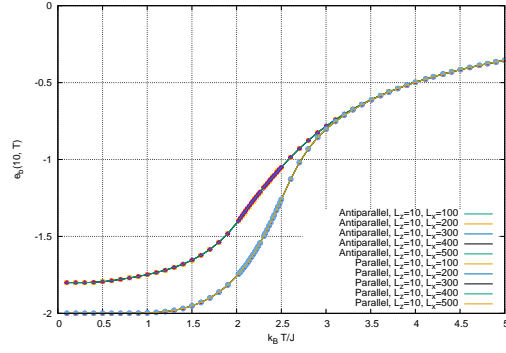
(a) $L_z = 4$



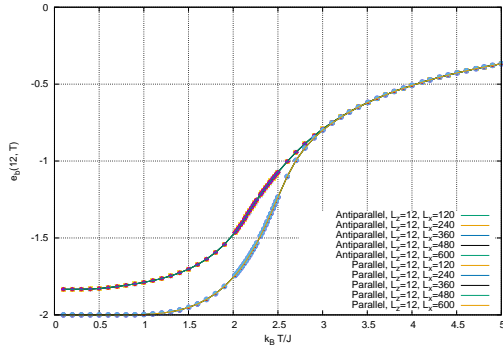
(b) $L_z = 6$



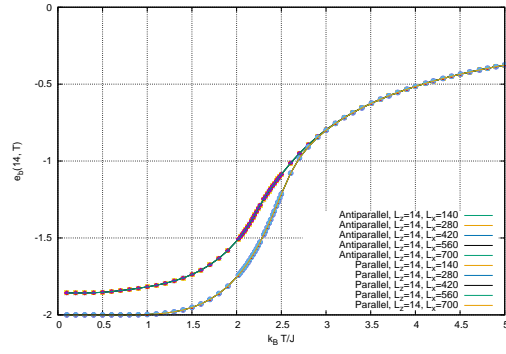
(c) $L_z = 8$



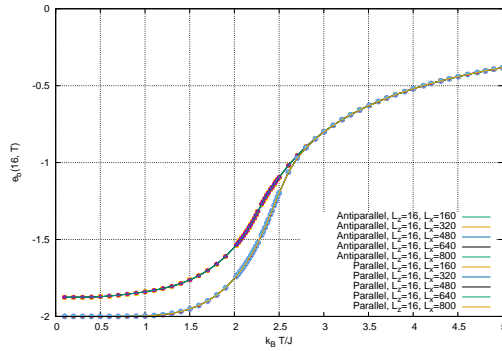
(d) $L_z = 10$



(e) $L_z = 12$

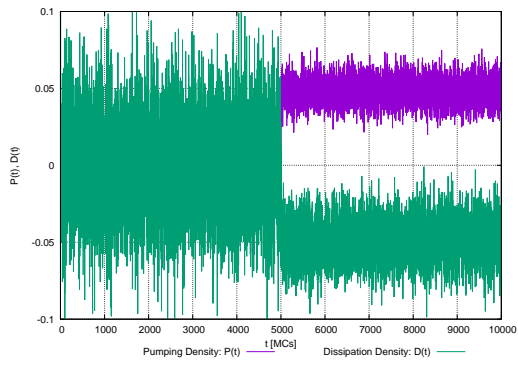


(f) $L_z = 14$

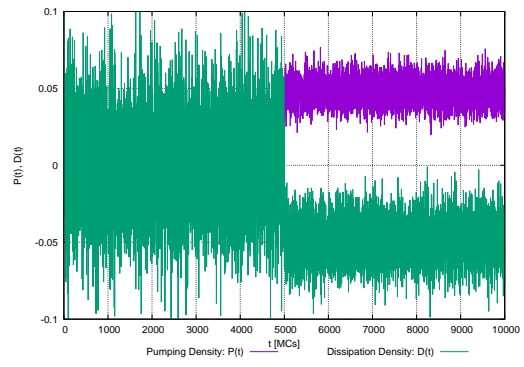


(g) $L_z = 16$

Figure B.2: Each data shows $E(L_x, L_z, T)/(L_x L_z)$ versus T .



(a) $T = 5.0$



(b) $T = 5.0$

Bibliography

- [1] Alfred Hucht. Non-equilibrium phase transition in an exactly solvable driven Ising model with friction. *Phys. Rev. E*, 80(6):061138, sep 2009.
- [2] Dirk Kadau, Alfred Hucht, and Dietrich E. Wolf. Magnetic Friction in Ising Spin Systems. *Phys. Rev. Lett.*, 101(13):137205, sep 2008.
- [3] M. P. Magiera, L. Brendel, D. E. Wolf, and U. Nowak. Spin excitations in a monolayer scanned by a magnetic tip. *EPL (Europhysics Lett.)*, 87(2):26002, 2009.
- [4] Martin P. Magiera, Sebastian Angst, Alfred Hucht, and Dietrich E. Wolf. Magnetic friction: From Stokes to Coulomb behavior. *Phys. Rev. B*, 84(21):212301, dec 2011.
- [5] Martin P. Magiera, L. Brendel, D. E. Wolf, and U. Nowak. Spin waves cause non-linear friction. *Europhys. Lett.*, 95:17010, 2011.
- [6] Roy J. Glauber. Time-Dependent Statistics of the Ising Model. *J. Math. Phys.*, 4(2):294, 1963.